Struct Chem
DOI 10.1007/s11224-015-0597-5

ORIGINAL RESEARCH

NMR conformational analysis in solution of a potent class of cysteine proteases inhibitors

Archimede Rotondo[1] · **Roberta Ettari**[2] · **Silvana Grasso**[1] · **Maria Zappalà**[2]

Received: 13 April 2015 / Accepted: 30 April 2015

Abstract Conformational analysis of a potent class of cysteine protease inhibitors is thoroughly studied by NMR, in both, polar and apolar solvents to get a better insight over the known biological activity and migration through biological media. These molecules are composed by a benzodiazepine (BDZ) scaffold connected to a bromo-isoxazoline (IOX) ring through an alkyl spacer (AS) with up to four-carbon atoms. Data, supported by theoretical calculations at DFT level, reveal that both BDZ and IOX keep a pretty rigid and asymmetric conformation, so that four diastereo-atropisomers (two mirror-image couples) are generated. The relative stiffness of these substrates, maintained also in different solvents, is confirmed by: (a) remarkable separation of diastereotopic protons; (b) specific "through the space contacts" (NOESY); and (c) very good fitting of the coupling constants evaluations. The prototypic compound with the longer AS shows two main conformations and a certain dynamic freedom around the AS torsional angles close to IOX; according to our data, the AS length is not fundamental for the functional BDZ and IOX fitting into the macromolecular complex; however, it does play a crucial role to cross the parasite cell membranes.

Keywords Proteases inhibitors · ^{1}H, ^{13}C, ^{15}N NMR · Solution chemical structure · Conformational analysis

Introduction

Neglected tropical diseases (NTDs) are a group of tropical infections, affecting more than 1.4 billion people [1], in this context one of the most relevant disease is the Human African Trypanosomiasis (HAT), also known as sleeping sickness. HAT is caused by parasites of *Trypanosoma* genus, two of which are able to transmit the disease to humans: *T. brucei gambiense*, and *T. brucei rhodesiense*, which cause the chronic and acute form of the disease, respectively [2]. At present, there are only a few available drugs for HAT treatment: suramine and pentamidine which are active on the first (haemolymphatic) stage of the disease, while the second-stage active drugs melarsoprol and eflornithine show many disadvantages that limit their use: the arsenical derivative causes encephalopathy in 5–10 % of treated patients, while eflornithine is active only against *T. brucei gambiense.* In addition, the therapy is very expensive and difficult to administer, requiring hospitalization [3]. Taking into consideration all these reasons, there is an urgent need to identify promising targets and to develop new drugs. To address this need, we focused our attention on rhodesain, a clan CA, family C1 (papain family) cysteine protease that plays essential roles in *T. b. rhodesiense* life cycle [4]; specifically, it is required to cross the blood–brain barrier (BBB), leading to the second lethal stage of the disease; moreover, it plays a fundamental role in evading the host immune system.

In this context, our research group has been involved in the last years into the development of cysteine protease inhibitors for the treatment of NTDs [5–14]. In particular,

Electronic supplementary material The online version of this article (doi:10.1007/s11224-015-0597-5) contains supplementary material, which is available to authorized users.

✉ Archimede Rotondo
arotondo@unime.it

[1] Department of Chemical Sciences, University of Messina, via D'Alcontres 31, 98166 Messina, Italy

[2] Department of Drug Sciences and Products for Health, University of Messina, Viale Annunziata, 98168 Messina, Italy

Published online: 16 May 2015

Table 1 Activity of the peptidomimetics **1–3** towards rhodesain, FP-2, *T.b.brucei* and *P. falciparum*

	Comp	Rhodesain	Falcipain-2	*T. b. brucei*	*P. falciparum*
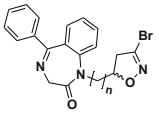 (±)-1 n=2 (±)-2 n=3 (±)-3 n=4	(±)-**1**	2.85	4.86	>40	1.17
	(±)-**2**	3.33	4.49	>40	1.59
	(±)-**3**	2.44	10.6	12.22	0.71

we focused our attention on the design of peptidomimetics whose use, with respect to peptides, is particularly advantageous in terms of potency and selectivity, as widely demonstrated in these years by our group within the development of protease inhibitors [15–19]. More recently, we developed novel peptidomimetics with a 3-bromoisoxazoline group (IOX) as innovative warhead, able to react with the active site cysteine of rhodesain, thus leading to a reversible inhibition of the target enzyme [20, 21]. Promising inhibitors were obtained by coupling a 1,4-benzodiazepine (BDZ) scaffold, a recognition motif widely employed by our group, with IOX, connected by means of an aliphatic chain (AC) of different length (2–4 carbon atoms). When tested against rhodesain compounds **1–3** showed K_i values in the range 2.44–3.33 μM, with the inhibitor **3**, with the longest AC, endowed with an antitrypanosomal activity of 12.22 μM with respect to the poor activity of the homologous molecules **1** and **2**. At the same time, compounds **1–3** were tested on falcipain-2 (FP-2), a cysteine protease of *P. falciparum*, belonging like rhodesain to papain family. The results of this investigation clearly pointed out that, while compounds **1** and **2** showed a better binding affinity with respect to compound **3** (see Table 1); however, also in this case, the isoxazoline derivative **3** showed the best antiplasmodial activity ($IC_{50} = 0.71$ μM), highlighting its strong ability to cross the parasite cell membrane. Starting from these considerations, we decided to perform an NMR structural characterization and conformational analysis of the three inhibitors **1–3**, in order to better correlate their biologically active conformation to their antiparasitic activity.

Results and discussion

Structural considerations concerning the investigated compounds are a key step towards the understanding of their promising antiparasitic activity. Compounds **1–3** are composed by the 5-substituted IOX warhead connected to the BDZ scaffold through an AS ranging from two to four C atoms. Spectral data concerning the six samples of **1–3**, dissolved either in $CDCl_3$ or CD_3OD, reveal that there are not noteworthy spectral differences among these; therefore, BDZBuIOX (**3**), with the systematic name 1-[4-(3-bromo-4,5-dihydro-1,2-oxazol-5-yl)butyl]-5-phenyl-1,3-dihydro-2*H*-1,4-benzodiazepin-2-one, is chosen as the most representative as it issues the best biological response, and we will mainly focus on this structure with the systematic labelling indicated in Scheme 1.

1,4-Benzodiazepine, such as diazepam, is among the most important scaffolds in medicinal chemistry, being considered "privileged structures" [22]. Despite the absence of a stereogenic centre, the seven-membered ring assumes two chiral boat conformations being 3-CH_2 proS over the benzo-fused ring, or far away from it. Traditionally, these two conformational enantiomers were indicated with the P and M notation (helicoidal descriptors of endocyclic dihedral angles), respectively (Fig. 1) [23, 24]. It is also known that racemization rate is tuned by the substituent on the N1 position which at least might prevent the process allowing asymmetric resolution even for preparative purposes [25, 26] and M to P interconversion needs very high temperatures to fall within NMR timescales (spectral line broadenings) [22, 26].

Conformational analysis

Conformational analysis of biologically active compounds is by itself a fundamental step within the whole knowledge about the interaction mechanisms occurring in the

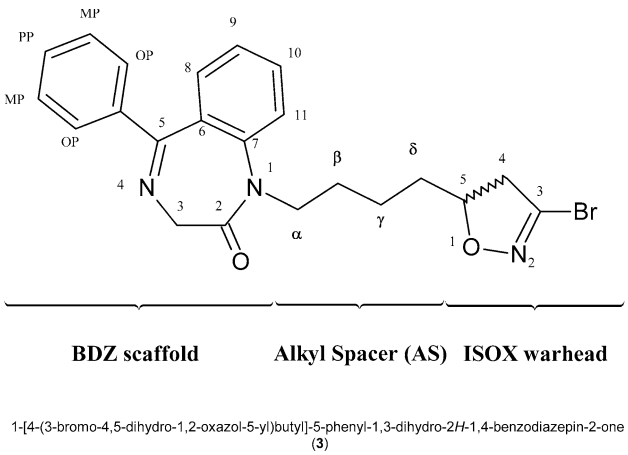

1-[4-(3-bromo-4,5-dihydro-1,2-oxazol-5-yl)butyl]-5-phenyl-1,3-dihydro-2*H*-1,4-benzodiazepin-2-one (**3**)

Scheme 1 Molecular representation of **3** with the labelling scheme used in the text

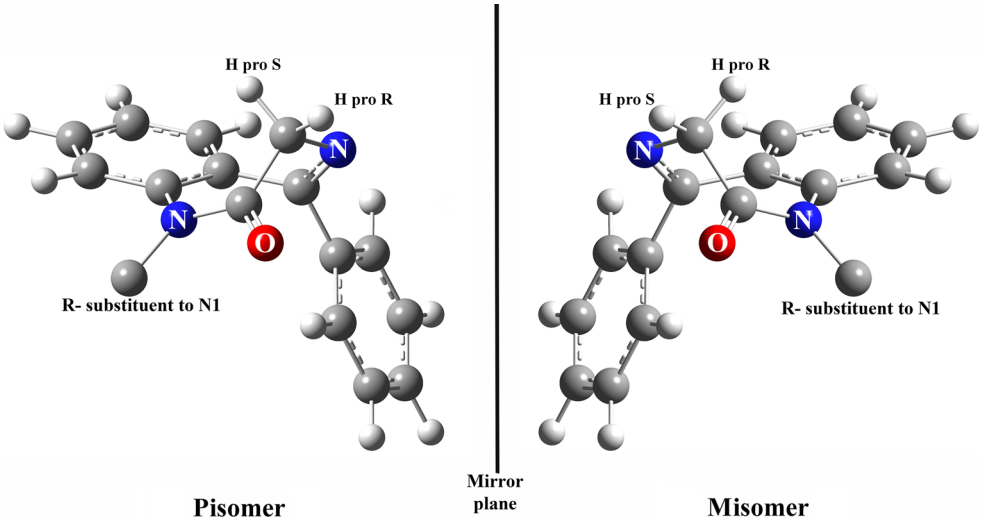

Fig. 1 Structural asymmetric conformations of BDZ labelled with helicoidal descriptors *P* and *M*. In the case of **1–3,** the quite big *R* substituent increases the M to P interconversion barrier

chemistry of life [27]. Moreover, many chemicals travelling inside biological systems pass through different environments sometimes undergoing conformational changes [28]. Being compound **3** very soluble in chloroform, it was straightforward to perform the first NMR analysis in this solvent (Fig. 2b). From the ^{1}H NMR spectrum, it was immediately clear that, beyond the presence of the chiral centre, all diastereotopic CH_2 methylene signals look definitely split. We have also observed that compound **3** is soluble in CD_3OD (4–6 mg/mL, temperature-dependent) so that we could run a complete NMR characterization also in this "polar-like" medium (Fig. 2a). Unlike other assessed cases [28], the overall spectral pattern does not change keeping apart the proton diastereotopic resonances (Fig. 2):

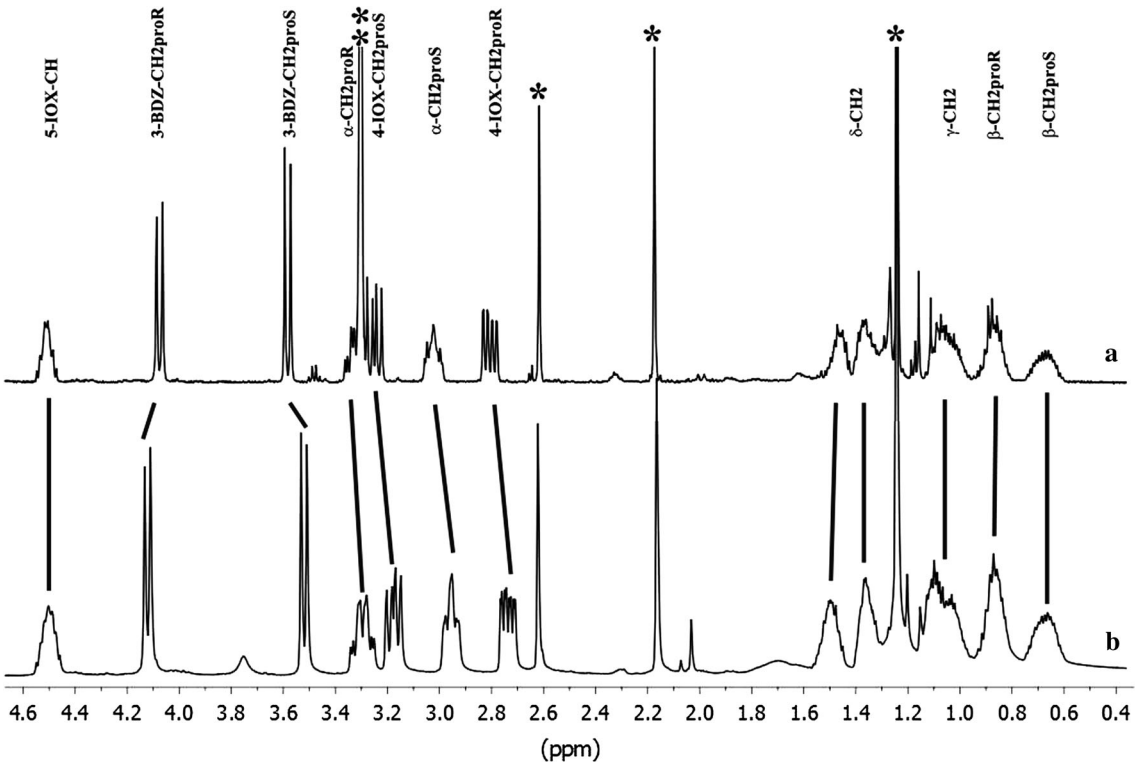

Fig. 2 ^{1}H NMR profile of the aliphatic region for compound **3**: **a** in the CD_3OD polar solvent; **b** in the less polar $CDCl_3$ environment. The *assignment* referred to the P–S isomer (see Table 2) is also reported, whereas peaks with * label are impurities and the ** resonance is the residual hydrogenated solvent signal

Table 2 Assigned ^{1}H and parent ^{13}C resonances for the samples **1–3** analysed in apolar solvent (**A**) $CDCl_3$ and in (P) polar solvent CD_3OD

Compound		BDZEtIOX (1)				BDZPrIOX (2)				BDZBuIOX (3)			
Moiety	Chem. Group	^{1}H in A	^{1}H in P	^{13}C in A	^{13}C in P	^{1}H in A	^{1}H in P	^{13}C in A	^{13}C in P	^{1}H in A	^{1}H in P	^{13}C in A	^{13}C in P
BDZ group	3-CH_2 proR	4.14	4.09	50.5	51.4	4.14	4.09	50.5	51.4	4.15	4.08	50.5	51.3
	3-CH_2 proS	3.54	3.61			3.54	3.61			3.54	3.59		
	8-CH	8.04	7.96	127.0	127.5	8.03	7.95	127.0	127.5	8.02	7.95	126.9	127.3
	9-CH	7.48	7.55	127.4	128.4	7.48	7.54	127.3	128.3	7.47	7.52	127.2	128.2
	10-CH	7.54	7.62	131.1	132.2	7.53	7.61	131.0	132.1	7.51	7.59	130.8	132.0
	11-CH	7.26	7.45	123.6	124.8	7.24	7.44	123.5	124.8	7.22	7.40	123.1	124.6
Ph	o–CH	7.31	7.27	126.6	127.4	7.30	7.26	126.5	127.4	7.29	7.26	126.3	127.2
	m-CH	7.34	7.38	128.9	129.8	7.34	7.38	128.7	129.7	7.31	7.37	128.7	129.6
	p–CH	7.35	7.40	129.7	130.7	7.35	7.40	129.8	130.8	7.32	7.36	129.6	130.6
Alkyl Spacer	α-CH_2 proR	3.66	3.60	45.3	45.6	3.33	3.40	48.6	49.0	3.30	3.33	48.4	49.3
	α-CH_2 pros	3.17	3.16			3.01	3.09			2.96	3.03		
	β-CH_2 proR	0.85	1.00	32.7	33.2	0.81	0.90	22.9	23.5	0.87	0.87	26.5	27.3
	β-CH_2 pros	0.71	0.94			0.65	0.78			0.67	0.68		
	γ-CH_2 proR	–	–	–	–	1.31	1.33	31.9	32.6	1.02	1.04	22.5	23.3
	γ-CH_2 pros	–	–			1.31	1.34			1.08	1.07		
	δ-CH_2 proR	–	–	–	–	–	–	–	–	1.50	1.47	34.3	35.0
	δ-CH_2 pros	–	–			–	–			1.37	1.38		
IOX	5-CH	4.39	4.26	79.6	81.0	4.42	4.44	81.4	83.0	4.50	4.52	81.7	83.0
	4-CH_2 proR	2.40	2.59	46.6	47.2	2.62	2.71	46.4	46.8	2.74	2.81	46.4	46.8
	4-CH_2 proS	3.12	3.19			3.11	3.20			3.17	3.26		

The assignment is made for the **3** P,S isomer considering the homologous protons (please note that some of the proR/S labels would change for compounds **1–3**)

this suggests there is not a dramatic effect of the solvent on the conformational features of **1**–**3**. Usually, this effect is remarkable in the case of rather rigid conformations; consistently, after the complete and total assignment of the ^{1}H and ^{13}C signals, it was possible, in both solvents, to observe specific scalar (dihedral angles evaluation) and dipolar couplings ("through the space" information) matching conformations with rather limited degrees of freedom. Measured scalar and dipolar coupling occurring between geminal protons are obvious and taken as a reference and will not be further mentioned or drown in order to simplify the discussion.

Another important feature of the ^{1}H profiles is the pronounced line broadening involving especially resonances close to the 5-IOX chiral centre; a careful analysis of the ^{13}C traces together with HSQC also reveal the 1:1 splitting of the related parent ^{13}C atoms. This accounts for the very rigid conformation of the asymmetric M and P BDZ joined to the 5-IOX asymmetric centre; it generates an atropodiastereomeric mixture (say M–S and P–S together with their respective mirror images P–R and M–R), whose very slight differences are reasonably perceived far away from the BDZ fragment and close to the 5-IOX centre. From now on, the structural considerations will be discussed for the P–S form to be eventually extended to the other isomers. The stiffness of BDZ is further confirmed by the NOE contacts, between the BDZ-8-CH and BDZ-11-CH with the BDZ-3-CH_2 at around 3.55 ppm (assigned as proS in the case of Fig. 3).

Further NMR considerations

Looking at the assignments (Table 2), it is immediately clear that all of the AS-CH_2 in the β position present two different signals at very low frequencies (0.64–0.95 ppm) regardless the length of the spacer. This is a clear evidence of a strong shielding anisotropic effect on the second methylene group imposed by a specific arrangement. Albeit pretty close, these two resonances give different Nuclear Overhauser Effect (NOE) being the β-CH_2proS, specifically close to the α-CH_2proR and the β-CH_2proR closer to the α-CH_2proS. These evidences also fit the great ^{3}J coupling constants (≈7 Hz) between α-CH_2proS and β-CH_2proS, and between α-CH_2proR and β-CH_2proR against the small values (≈1 Hz) for the crossing over homologous ones ([β-CH_2proS/α-CH_2proR] and [β-CH_2proR/α-CH_2proS]); according to the Karplus law, indeed [29, 30], coupling constants strongly support the typical staggered-trans conformation around the αC-βC dihedral angle already envisaged by the nuclear contacts. Nonetheless, NOE in any solvent, show close contacts between the BDZ-11-CH and both of the two α-CH_2proS and β-CH_2proS (far away from each other). As the simultaneous presence of these space contacts is physically impossible (Fig. 3), provided that the dihedral angle around αC-βC is rather locked, experimental data unambiguously show the presence of two rotamers around the N-αC dihedral angle in fast equilibrium within the NMR time scale. These two configurations lead to pseudo-axial or pseudo-equatorial orientation of the AS respect to the average mean plane of the BDZ (Fig. 4). DFT optimizations assessed that these conformations, as well as the different diastereoisomers, are energetically close (Table 3); therefore, it is reasonable to think they equally

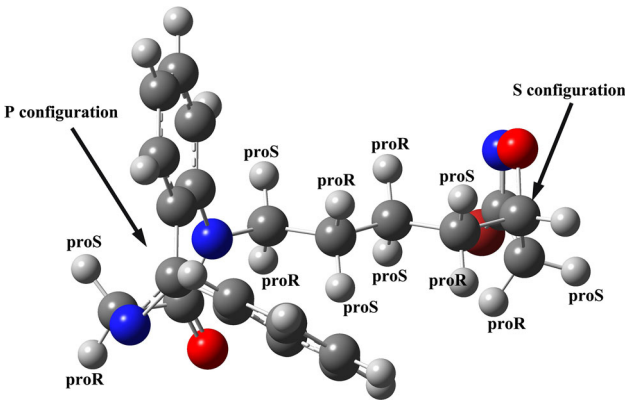

Fig. 3 Ball and stick 3D model of **3 P–S** diastereo-atropisomer with axial orientation of the AS; P and S labels, as well as proR and proS, are indicated on the specific positions according to the conventional use

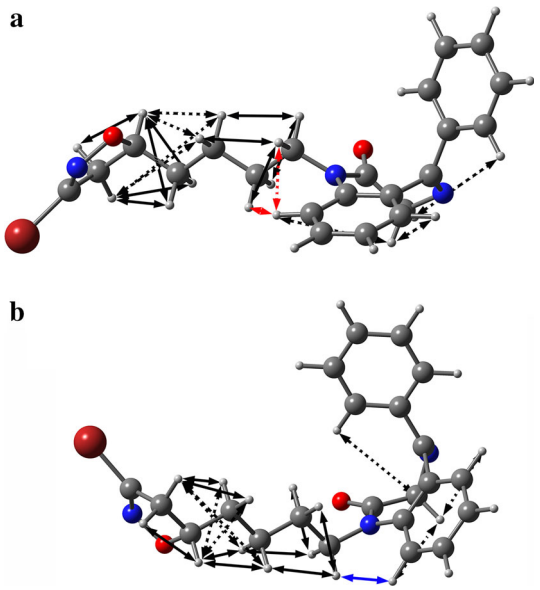

Fig. 4 3D models of **P–S** isomer of compound **3**: double-headed harrows evidence the most non-geminal through the space vicinities: *grey/coloured* connections are reasonable just for **a** pseudo-equatorial or just for **b** pseudo-axial rotamer. *Dashed lines* indicate weak signals due to: (**a**) long-range contacts, (**b**) averaged contacts due to conformational freedom

Table 3 Calculated energies of configurational and conformational isomers of **3,** at DFT level, with LSDA method using Gaussian 6-3-1 basis sets

Isomeric form	ΔE (kJ/mol)	Dipolar moment (D)
3 S-P-pseudo-equatorial AS	0	1.74
3 R-M-pseudo-equatorial AS	0	1.74
3 S-P-pseudo-axial AS	+5.05	8.58
3 R-M-pseudo-axial AS	+5.05	8.58
3 S-M-pseudo-equatorial AS	+3.68	7.96
3 R-P-pseudo-equatorial AS	+3.68	7.96
3 S-M-pseudo-axial AS	+2.35	3.97
3 R-P-pseudo-axial AS	+2.35	3.97

Couples of mirror images display obviously the same properties

share almost the entire molecular population. In summary, the pseudo-axial arrangement, with α-CH_2proS very close to the aromatic BDZ-11-CH, accounts for the great anisotropic shielding effect sensed by the β-methylene group as it is permanently facing both the aromatic BDZ rings (Fig. 4b); on the other hand, pseudo-equatorial orientation matches the intense NOE cross-peaks between β-CH_2proS and the BDZ-11-CH and the weaker NOE between α-CH_2proR and the BDZ-11-CH (Fig. 4a).

The staggered-trans conformation seems to be assumed also by the next alkyl connection as demonstrated by the definite NOE 1,3 contacts (α-CH_2proS/γ-CH_2proR and α-CH_2proR/γ-CH_2proS; see Fig. 4); however, starting from the β-position the relatively weak but detectable 1,2 and 1,3 methylene vicinities witness that dihedral angle around γC-δC is endowed with a certain degree of freedom.

Finally, as expected by the model, the IOX ring is almost planar. Coupling constants between the two IOX-4-CH_2 and the stereogenic IOX-5-CH are pretty big and very similar to each other (9 and 10 Hz); according to the Karplus law, dihedral angles are either close to 0° or around 180°, therefore, albeit the two-carbon atoms are sp^3; nonetheless, the planar conformation clearly driven by the conjugation of the heterocyclic segment prevents possible envelope-like folding. For the given configuration S, the IOX-4-CH_2 proS can be assigned considering the strong dipolar coupling to the IOX-5-CH (dihedral angle close to 0°) together with the lack of other detectable vicinities. On the other hand, expectedly, the geminal IOX-4-CH_2 proR does not show NOE with IOX-5-CH (dihedral angle not far from 180°); but does present space contacts towards AS-δ and AS-γ methylene protons. Again the clear contacts of both spatially separated 5-IOX-CH and 4-IOX-CH_2proR towards δ-CH_2 protons; and, with a lesser intensity, towards the next and opposite γ-CH_2 (Fig. 4), warrantees free rotation around the (AS-δC)-(IOX-5-C) bond, with the most probable staggered-trans arrangement drawn in Fig. 4.

In conclusion provided, there are two specific rotameric conformations around the N-αC bond for **1–3**, the most conformational freedom is localized on the segment AS-γC-δC-5C which is specifically present in the compound **3**. Albeit it is usually obvious the free rotation around C–C bonds of alkyl chains, this is not the case because of the great steric hindrance between two big and very rigid heterocyclic moieties (BDZ and IOX). According to the differences into the activities of compounds **1–3** shown in Table 1, regardless the chemical affinity with the proteases, it is probable that the key dynamic role of the **3** butylic AS is played by crossing the biological barriers made by the pathogenic organisms. In this crucial step, BDZ and IOX might be dynamically kept in an advantageous position from each other, afterwards BDZ and IOX can easily accommodate into their biologically active molecular complex. Another important role to be mentioned is certainly played by both the BDZ and IOX stereogenic centres which probably lead to one over the four isomers particularly active into the macromolecular complex.

Experimental section

NMR

^{1}H, ^{13}C{^{1}H} and ^{15}N{^{1}H} NMR spectra of **1–3** were recorded on Bruker Avance 300 MHz NMR spectrometer equipped with a BBI probe and operating at frequencies of 300.13, 75.47, 30.42 MHz; many experiments were double checked on a Varian 500 MHz spectrometer equipped with a ONE_NMR probe and operating at 499.74, 125.73, 50.65 MHz, respectively. Compounds **1–3** were dissolved in 500 μL of $CDCl_3$ (10–20 mg) and in 500 μL of CD_3OD (saturated solution, about 10 mg/mL). The complete and unambiguous assignment is confirmed by homo-nuclear 2D-COSY and NOSY [31] and heteronuclear [32] ^{13}C{^{1}H}-HSQC, ^{13}C{^{1}H}-HMBC and ^{15}N{^{1}H}-HMBC experiments. Extended NMR data are reported (Tables 2; Fig. 2; supplementary material) in order to easily compare differences determined by the spacer or by the used solvent. We have chosen to present the ^{1}H, ^{13}C and ^{15}N chemical shifts (*cs*) in CD_3OD in order to reproduce a polar medium somewhat reminding a biological environment; other measurements, made in the more polar CD_3OH/H_2O 80/20 % mixture, demonstrated again there are not dramatic changes in the ^{1}H profile. Calibration was attained using as internal standard residual proton signal of the solvent (CD_2HOD quintet: $\delta = 3.31$ ppm; $CHCl_3$ $\delta = 7.26$ ppm and the ^{13}C solvent septuplet at $\delta = 49.0$ ppm and triplet $\delta = 79.0$, respectively) [33]. ^{15}N calibration was referred to the absolute frequency provided that the CH_3NO_2 as external standard was also calibrated (90 % CH_3NO_2 in CD_3OH $\delta = 380.5$ ppm)

[34]. The average distances are extracted by many 2D-NOSY and 1D-NOE experiments run at different mixing times [35] and used according to the two-spin-system approximation; experimental data are reported in the supplementary material, whereas the main relevant features are fully discussed in the experimental section.

Computer-aided analysis

Several NMR simulations, to confirm the correct assignment related to the specific 3D-structure, were run by the PERCH NMR software package (v. 2014.1, PERCH Solutions Ltd., Kuopio, Finland); as the diastereo-atropisomeric mixture hampered the perfect line fitting, we also used the manual best fitting of both PERCH and i-NMR (version 5.4.3 for Windows 7) software packages. All the shown molecular models are represented using Gaussian View or PERCH MMS belonging to Gaussian 03 [36] and PERCH software packages, respectively. Molecular optimizations well fitting the NMR data were run by PERCH models with simple molecular mechanics and later reviewed by Gaussian DFT calculations with the LSDA method with the G631 basis set. This level of calculation is considered reasonable according to: (a) the presence of elements belonging to the first raw except for the peripheral Bromine atom; (b) the affordable time-consuming calculations on a normal four processors PC. The output resulting file for structures of **3** (Table 3) are enclosed in the supplementary material.

Synthesis

The synthesis of the inhibitors (±)-**1**–**3,** was realized as previously described by our group [21], by treating the benzodiazepine **4** with the bromo-alkenes **5**–**7**, in the presence of sodium hydride, to obtain intermediates **8**–**10**. The terminal olefins **8**–**10** were, in turn, used as dipolarophile to react in a 1,3-dipolar cycloaddition with the 1,3-dipole bromonitrile oxide, generated in situ by dehydrohalogenation of the stable precursor dibromoformaldoxime, to afford the isoxazoline derivatives (±)-**1**–**3** (Scheme 2).

Conclusions

Because of the tight relationship between compounds used in medicinal chemistry and the nature of their functional and structural features [28, 37], we decided to run specific structural analysis in solution concerning molecules endowed with pharmaceutical properties. A specific class of compounds, with the "privileged" BDZ scaffold linked to the IOX moiety through an AS with two- to four-carbon atoms, was carefully analysed in solution by NMR techniques. Studies were extended to different solvents in order to detect possible differences sometimes affecting drug candidates [29]. In this case though, the pretty rigid conformation of the BDZ structure and the imposed quasi-planar conformation of the IOX, hamper most of the conformational arrangements.

Moreover, ^{1}H line broadening and ^{13}C splitting of the signals around the 5-IOX stereogenic centre clearly account for the presence of diastereo-atropisomers being the asymmetric BDZ folded either in the P or in the M mode against the other traditional 5C-IOX (S or R) stereogenic centre.

Conformational analysis evidences that the dihedral angle αC-βC on the AS is pretty locked, whereas two main conformations are detected around the N-αC dihedral angle yielding the completely different pseudo-axial or pseudo-equatorial orientation of the AS-IOX terminus. This allows just a limited degree of freedom for **1** and **2** whose short AS tie causes steric bumping between BDZ and IOX; however, **3** with the butyl AS owns much more flexibility because of the conformational freedom around AS dihedral angles closer to the IOX. The drawn structural models fully match all the NMR data (very big amount of information) unambiguously confirming the conformational analysis of compound **3**.

Starting from the consideration that compound **3** was shown to possess the best activity against both *T. b. brucei* and *P. falciparum,* respectively, in the low micromolar and submicromolar range, we can assume that beyond the importance of the BDZ scaffold, which acts as recognition motif, and of the IOX which behaves as warhead, a key role in the ability to cross the parasite cell membranes of inhibitor **3** must be attributed to the AS. On this regard, while a two- or three-carbon-atom AS is responsible for a

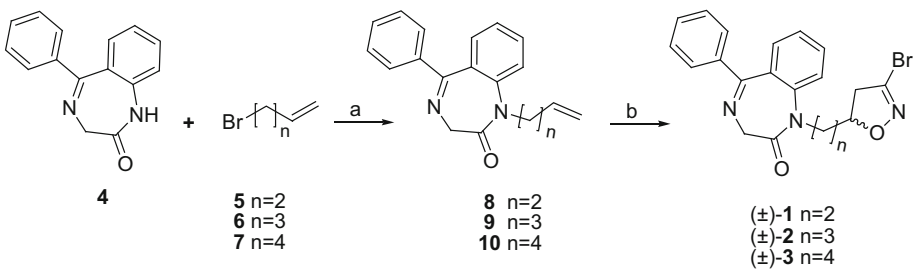

Scheme 2 Reagents and conditions: **a** NaH, DMF, 0 °C, N_2, 1 h, then **5**–**7**, rt, 12 h; **b** DBF, $NaHCO_3$, EtOAc, 12 h

limited degree of freedom of homologous compounds **1** and **2,** on the contrary, a four-carbon atoms AS contributes to an enhanced flexibility of compound **3** which accounts for its great antiparasitic activity reported in Table 1.

Looking at the modelling of similar inhibitors [14], we might suppose that the pseudo-equatorial conformation is assumed in the active macromolecular complex; however, the conformational freedom is kinetically crucial to fit the molecule in its binding site [28]. Another important role is probably played by the traditional IOX stereogenic centre and by the BDZ atropo-stereogenic centre which might reasonably give to one configurational substrate (over four) specifically active towards the biological targets. This paper is the beginning molecular approach to get more clues about the mechanism of action of specific drug candidates; thus, it might pave the way towards the knowledge of both the interaction with macromolecules and specific biological pathways undertaken by these investigated substrates.

Acknowledgments We gratefully thank the MIUR (Ministero dell'Istruzione, Università e Ricerca) for supporting our research.

References

1. http://www.whoint/neglected_diseases/diseases/en/
2. Barrett MP, Burchmore RJS, Stich A, Lazzari JO, Frasch AC, Cazzulo JJ, Krishna S (2003) Lancet 362:1469–1480
3. http://www.whoint/mediacentre/factsheets/fs259/en/
4. Ettari R, Tamborini L, Angelo IC, Micale N, Pinto A, De Micheli C, Conti P (2013) J Med Chem 56:5637–5658
5. Micale N, Kozikowski AP, Ettari R, Grasso S, Zappalà M, Jeong J-J, Kumar A, Hanspal M, Chishti AH (2006) J Med Chem 49:3064–3067
6. Ettari R, Nizi E, Di Francesco ME, Dude MA, Pradel G, Vicik R, Schirmeister T, Micale N, Grasso S, Zappalà M (2008) J Med Chem 51:988–996
7. Ettari R, Nizi E, Di Francesco ME, Micale N, Grasso S, Zappalà M, Vičík R, Schirmeister T (2008) Chem Med Chem 3:1030–1033
8. Ettari R, Micale N, Schirmeister T, Gelhaus C, Leippe M, Nizi E, Di Francesco ME, Grasso S, Zappalà M (2009) J Med Chem 52:2157–2160
9. Micale N, Ettari R, Schirmeister T, Evers A, Gelhaus C, Leippe M, Zappalà M, Grasso S (2009) BMC 17:6505–6511
10. Bova F, Ettari R, Micale N, Carnovale C, Schirmeister T, Gelhaus C, Leippe M, Grasso S, Zappalà M (2010) BMC 18:4928–4938
11. Ettari R, Zappalà M, Micale N, Schirmeister T, Gelhaus C, Leippe M, Evers A, Grasso S (2010) Eur J Med Chem 45:3228–3233
12. Ettari R, Zappalà M, Micale N, Grazioso G, Giofrè S, Schirmeister T, Grasso S (2011) Eur J Med Chem 46:2058–2065
13. Ettari R, Micale N, Grazioso G, Bova F, Schirmeister T, Grasso S, Zappalà M (2012) Chem Med Chem 7:1594–1600
14. Grazioso G, Legnani L, Toma L, Ettari R, Micale N, De Micheli C (2012) JCAMD 26:1035–1043
15. Ettari R, Bonaccorso C, Micale N, Heindl C, Schirmeister T, Calabrò ML, Grasso S, Zappalà M (2011) Chem Med Chem 6:1228–1237
16. Micale N, Ettari R, Lavecchia A, Di Giovanni C, Scarbaci K, Troiano V, Grasso S, Novellino E, Schirmeister T, Zappalà M (2013) Eur J Med Chem 64:23–34
17. Scarbaci K, Troiano V, Micale N, Ettari R, Tamborini L, Di Giovanni C, Cerchia C, Grasso S, Novellino E, Schirmeister T, Lavecchia A, Zappalà M (2014) Eur J Med Chem 76:1–9
18. Micale N, Scarbaci K, Troiano V, Ettari R, Grasso S, Zappalà M (2014) Med Res Rev 34:1001–1069
19. Troiano V, Scarbaci K, Ettari R, Micale N, Cerchia C, Schirmeister T, Novellino E, Grasso S, Lavecchia A, Zappalà M (2014) Eur J Med Chem 83:1–14
20. Ettari R, Tamborini L, Angelo IC, Grasso S, Schirmeister T, Lo Presti L, De Micheli C, Pinto A, Conti P (2013) Chem Med Chem 8:2070–2076
21. Ettari R, Pinto A, Tamborini L, Angelo IC, Grasso S, Zappalà M, Capodicasa N, Yzeiraj L, Gruber E, Aminake MN, Pradel G, Schirmeister T, De Micheli C, Conti P (2014) Chem Med Chem 9:1817–1825
22. Evans BE, Rittle KE, Bock MG, Di Pardo RM, Freidinger RM, Whitter WL, Lundell GF, Veber DF, Anderson PS, Chang RSL, Lotti VJ, Cerino DJ, Chen TB, Kling PJ, Kunkel KA, Springer JP, Hirschfield J (1988) J Med Chem 31:2235–2246
23. Linscheid P, Lehn JM (1967) Bull Chim Soc Fr 3:992–997
24. Carlier PR, Zhao H, De Guzman J, Lam PCH (2003) J Am Chem Soc 125:11482–11483
25. Carlier PR, Zhao H, MacQuarrie-Hunter SL, De Guzman JC, Hsu DC (2006) J Am Chem Soc 128:15215–15220
26. Gilman NW, Rosen P, Earley JV, Cook C, Todaro LJ (1990) J Am Chem Soc 112:3969–3978
27. Höög C, Rotondo A, Johnston BD, Pinto BM (2002) Carbohydr Res 337:2023–2036
28. Rotondo A, Ettari R, Zappala M, De Micheli C, Rotondo E (2014) J Mol Struct 1076:337–343
29. Karplus M (1963) J Am Chem Soc 85:2870–2871
30. Minch MJ (1994) Concept Magn Res 6:41–56
31. Wagner R, Berger S (1996) J Mag Res 123A:119–121
32. Willker W, Leibfritz D, Kerssebaum R, Bermel W (1993) Magn Res Chem 31:287–292
33. Gottlieb HE, Kotlyar V, Nudelman A (1997) J Org Chem 62:7512–7515
34. Harris RK, Becker ED, Cabral De Menezes SM, Goodfellow R, Granger P (2001) Pure Appl Chem 73:1795–1818
35. Markley JL, Bax A, Arata Y, Hilbers CW, Kaptein R, Sykes BD, Wright PE, Wüthrich K (1998) J Mol Biol 280:933–952
36. Frisch MJ, Trucks GW, Schlegel HB, Scuseria GE, Robb MA, Cheeseman JR, Montgomery J, Vreven T, Kudin KN, Burant JC, Millam JM, Iyengar SS, Tomasi J, Barone V, Mennucci B, Cossi M, Scalmani G, Rega N, Petersson GA, Nakatsuji H, Hada M, Ehara M, Toyota K, Fukuda R, Hasegawa J, Ishida M, Nakajima T, Honda Y, Kitao O, Nakai H, Klene M, Li X, Knox JE, Hratchian HP, Cross JB, Adamo C, Jaramillo J, Gomperts R, Stratmann RE, Yazyev O, Austin AJ, Cammi R, Pomelli C, Ochterski JW, Ayala PY, Morokuma K, Voth GA, Salvador P, Dannenberg JJ, Zakrzewski VG, Dapprich S, Daniels AD, Strain MC, Farkas O, Malick DK, Rabuck AD, Raghavachari K, Foresman JB, Ortiz JV, Cui Q, Baboul AG, Clifford S, Cioslowski J, Stefanov BB, Liu G, Liashenko A, Piskorz P, Komaromi I, Martin RL, Fox DJ, Keith T, Al-Laham MA, Peng CY, Nanayakkara A, Challacombe M, Gill PMW, Johnson B, Chen W, Wong MW, Gonzalez C, Pople JA (2004) Gaussian 03, Revision E01. Gaussian Inc., Pittsburgh
37. Johnson MA, Rotondo A, Pinto BM (2002) Biochemistry 41(7):2149–2157